Materials Advances

ROYAL SOCIETY OF CHEMISTRY

PAPER

View Article Online
View Journal | View Issue



Cite this: *Mater. Adv.*, 2022, 3, 2056

# Conductive gold nanoparticle assembly linked through interactions between the radical cations of ethylene- and propylene-3,4-dioxythiophene mixed tetramer thiolate†

Tohru Nishinaga, * Kazuki Matsuo, Tomoya Koizumi and Ken-ichi Sugiura

Received 5th June 2021,
Accepted 1st January 2022

DOI: 10.1039/d1ma00493j

rsc.li/materials-advances

A conjugated mixed tetramer consisting of ethylenedioxythiophene (EDOT (E)) and propylenedioxythiophene (ProDOT (P)) dimers ($E_2P_2$) with a methylthio end-capping group at the EDOT side was directly introduced *via* a thiolate linker on a gold nanoparticle (AuNP) surface covered with dodecylamine by a ligand exchange reaction. The molar fraction of the thiolate of $E_2P_2$ in the dodecylamine protecting group of AuNPs reached up to 0.35. Cyclic voltammetry of the AuNPs showed two couples of anodic and cathodic peaks due to the $E_2P_2$ moiety, suggesting that the radical cation of the $E_2P_2$ unit could be generated on the AuNPs. In practice, the formation of stable radical cations of $E_2P_2$ on the AuNPs was observed in dichloromethane by chemical oxidation with $AgSbF_6$. The conductivity of the drop-cast film of the neutral AuNPs was moderate ($\sim 10^{-4}$ S cm$^{-1}$), while the conductivity after doping with iodine vapor was increased to $\sim 10^{-2}$ S cm$^{-1}$. Similarly, the drop-cast film of the dichloromethane solution of the chemically oxidized AuNPs having an $E_2P_2$ radical cation moiety showed better conductivity than the iodine-doped film. Accordingly, the π-dimer between the $E_2P_2$ radical cation moieties on the neighboring AuNPs was considered to form an effective conduction path in the AuNP assembly.



## Introduction

Gold nanoparticles (AuNPs) have attracted growing interest because of their unique functions arising from the particle size and properties of the surrounding groups on the surface.[1] A wide range of applications in the fields of catalysis,[2] electronics,[3] photonics,[4] sensing,[5] and medicine[6] have been investigated. Furthermore, the facile preparation and post-modification methods of surface-decorated AuNPs are optimized for excellent efficiency. Particularly, practical applications in stretchable conductors[7] and electrodes in solution-processable transistors[8] were demonstrated based on the high electrical conductivity of citrate- and phthalocyanine-capped AuNP assemblies, respectively. The advantages of nanoparticle-based conductors are their solution processability and intrinsic ability for self-organization due to their spherical structure.

Switching the electrical conductivity of AuNP assemblies by external stimuli is an intriguing challenge. To this end, various AuNPs modified with π-conjugated oligomers and polymers having direct connections *via* thiolate,[9–15] phosphine,[16] or *N*-heterocyclic carbene[17] anchor groups were prepared. The conductivity switching behaviors derived from the changes in the effective conjugation path and length of the π-systems on the AuNPs have been shown. For example, a 25-fold enhancement of conductivity in a device using diarylethene-based AuNP assemblies was observed by photoirradiation.[12] Diarylethenes are well-known photochromic materials.[18] Ring closure at the dithienylethene moiety after irradiation results in a better conduction path between the AuNPs. In contrast, the conductivity of diphenylphosphinoterthiophene-capped AuNP assemblies showed an $\sim 10^3$-fold enhancement after electrochemical oxidation.[16] In this case, the direct linkage between AuNPs through sexithiophene was formed by the oxidative coupling reaction at the α-position of the terminal thiophene unit of the terthiophene moiety. Accordingly, the direct linkage of AuNPs with π-conjugated systems is considered to be effective for achieving higher conductivity. However, the formation of covalent bonds is an irreversible process that limits conductivity switching.

Another promising method to control the conductivity switching of AuNPs is the utilization of the face-to-face interaction between π-radical cations (π-dimer) as an emerging non-covalent interaction for self-assembly.[19,20] The π-dimer is believed to form effective conduction paths in conductive, positively charged (p-doped) π-conjugated polymers.[21,22] In particular, as models of p-doped states for the representative conductive polymers of polythiophenes, radical cation π-dimers

*Department of Chemistry, Graduate School of Science, Tokyo Metropolitan University, Hachioji, Tokyo 192-0397, Japan. E-mail: nishinaga-tohru@tmu.ac.jp*

† Electronic supplementary information (ESI) available: General methods, synthesis, computational methods, $^1$H and $^{13}$C NMR spectra, Fig. S1–S4, and Cartesian coordinates of the optimized structures of all calculated molecules. See DOI: 10.1039/d1ma00493j

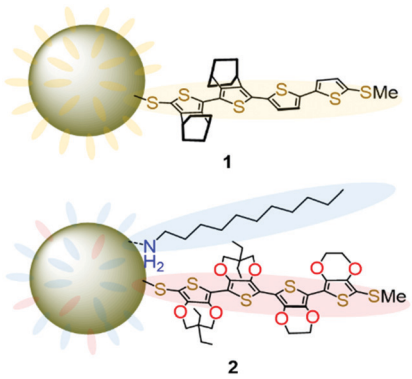


Fig. 1 Schematic representations of AuNPs **1** and **2**.

of various oligothiophenes were intensively investigated[23] and hence, they are considered to be one of the best candidates. Although most radical cations of oligothiophenes are prone to form covalently bonded dimers of the precursor oligomer in the condensed phase as previously utilized in the formation of the direct linkage between AuNPs,[16] appropriately modified oligothiophenes with a reversible one-electron oxidation have the potential to construct AuNP assemblies with redox-switchable conductivity.

We are interested in the basic properties and their applications to the supramolecular chemistry of the π-dimers of conjugated oligomer radical cations.[24–31] As such, AuNP **1** protected by thiolates of methylthio end-capped quaterthiophene partially annelated with bicyclo[2.2.2]octene units (Fig. 1) was prepared in our previous study.[32] The conductivity of the drop-cast film of **1** was below the measurement limit ($<10^{-6}$ S cm$^{-1}$) of the voltage–current monitor and interdigitated array (IDA) electrode used, while more than $10^4$-fold enhancement of conductivity was recorded after exposure of iodine vapor to the film. The desired π-dimer formation between the generated radical cations might lead to the formation of an effective conduction path. However, it could not be excluded that unwanted reactions such as the formation of other cationic states and/or bond formation at the β-position of the terminal thiophene ring also proceeded in the solid-state oxidation with $I_2$ vapor. Thus, it was difficult to provide further assessment of the ability of the π-dimer linker as a molecular wire. In this study, we prepared AuNP **2** covered with thiolates of the methylthio end-capped mixed tetramer consisting of ethylenedioxythiophene (EDOT (E)) and propylenedioxythiophene (ProDOT (P)) dimers in addition to dodecylamine capping groups (Fig. 1). The radical cation state of the mixed tetramer ($E_2P_2$) unit on the AuNP surface was stable in dichloromethane. Conductive AuNP assemblies were formed in the cast film prepared from the solution.

## Results and discussion

### Molecular design and synthesis

The electron-donating dioxy substituents in EDOT[33,34] and ProDOT[35,36] highly stabilized the radical cation state even with a relatively shorter oligomer length. Given that core-to-core (co)tunneling is considered to be the principal conduction mechanism of an AuNP assembly,[37] the use of oligomers with moderate length would be ideal. However, the synthesis of even tetramers of EDOT ($E_4$) without bulky end-capping groups is difficult owing to their poor solubility in common organic solvents. Alternatively, in the case of ProDOT, solubilizing side chains can be introduced in a symmetrical manner at the central carbon in the propylene constituent.[38] However, in our previous studies, we have found that the methylthio-end-capped tetramer of ProDOT ($P_4$) with a dihexyl side chain (**3**) does not have π-dimerization ability in the radical cationic state[35] partly owing to the intermolecular steric repulsion between the side chains. In contrast, we have also found that the combined EDOT–ProDOT mixed tetramer **4a** having the $E_2P_2$ structure with a methylthio end-capping group at both ends can form a radical cation π-dimer.[28] Furthermore, significant exchange interactions between nitronyl nitroxide spin labels through the π-dimers of $E_2P_2$ radical cations were proved in a later study.[30] This proposed that the ability of the π-dimer as a molecular wire is comparable or even superior to that of covalently linked conjugated oligomers. Thus, we chose thiolate of **4** as the surrounding group of AuNPs.

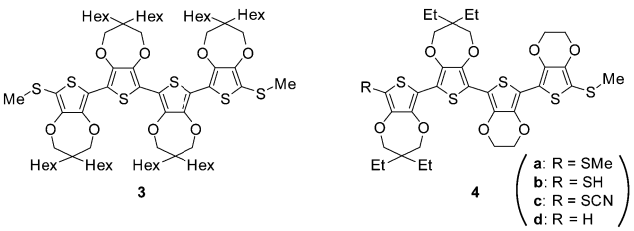


For the synthesis of the precursor thiol **4b**, the reduction of thiocyanate **4c** is a convenient process. Since we had already prepared the precursor **4d**,[30] we first attempted thiocyanation of **4d** using potassium thiocyanide and bromine, as in the case of the previous synthesis of **1**.[32] However, the reaction presented a complex mixture (Scheme 1a). Probably, **4d** suffered from undesired one-electron oxidation with $Br_2$ (reduction potential +0.07 V *vs.* Fc/Fc$^+$),[39] because the $E_2P_2$ moiety should have a lower oxidation potential judging from that for **4a** (−0.11 V *vs.* Fc/Fc$^+$)[28] due to multiple electron-donating oxy-substituents. Thus, we conducted thiocyanation of **4d** with *n*-BuLi, zinc thiocyanate, and *N*-chlorosuccinimide (NCS)[40] instead (Scheme 1b). After the thiocyanation, the $^1$H NMR signal of the terminal thiophene proton of **4d** ($\delta$ 6.37 ppm)[30] disappeared, while the characteristic $^{13}$C NMR signal of cyanide carbon was observed at 93.3 ppm. The yield (54%) was moderate, mainly because of the difficulty of the first lithiation step of

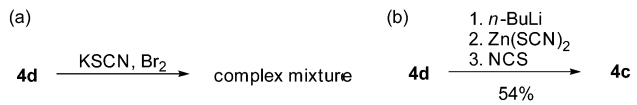


Scheme 1 Synthesis of **4c**.

the electron-rich $E_2P_2$ unit. Thus, some unreacted **4d** was recovered under these basic conditions.

In the previous synthesis of AuNPs **1**,[32] the precursor thiol was prepared through the reduction of thiocyanate with lithium aluminum hydride (LAH). The product was tolerant to oxidation during the work-up procedure using hydrochloric acid and ether in air. In the presence of this thiol, the Brust method,[41] which involved the reduction of tetrachloroauric(III) acid with sodium borohydride ($NaBH_4$), was applied to produce **1**. However, thiol **4b** was observed to be air-sensitive and the standard work-up after the reaction of **4c** with LAH produced a mixture which included the corresponding disulfide dimer based on the mass spectra and unidentified by-products (Scheme 2a). Therefore, we chose the ligand exchange reaction of AuNPs (~2.5 nm particle size) capped with dodecylamine (DDA) (**AuNPs–DDA**)[42] with *in situ* generated **4b** under a nitrogen atmosphere (Scheme 2b). The reaction was conducted in toluene, and therefore, soluble tetrabutylammonium borohydride was used as the reducing agent instead of $NaBH_4$. In this reaction, the rate of replacement of the DDA ligands with the thiolate of **4** seemed to be saturated in the middle stage. The molar fraction of the thiolate, including the remaining DDA on AuNPs after 24 h, reached up to ~0.35, based on a rough estimation of the $^1$H NMR spectra (see Fig. S1 in the ESI†). However, the precise control of the reaction rate was difficult because of the air sensitivity of **4b**, and the molar fraction was varied from 0.15 to 0.35. Hereafter, these AuNPs will be designated as **2**. The $^1$H NMR signals of the oligothiophene moiety in **2** and the alkyl chains of DDA broadened mainly due to the restricted mobility of these moieties on the AuNP surface in the solution. AuNP **2** was observed to be stable in air. Accordingly, once the thiolate coordinated to the AuNP surface, the formation of the disulfide, as observed in the attempted synthesis of **4b**, was suppressed.

### Basic properties of AuNPs 2

The electronic absorption spectra of AuNPs **2** in dichloromethane are shown in Fig. 2 together with those of **4c** and **AuNPs–DDA** for comparison. The absorption maximum of **4c** was observed at 443 nm with the vibrational fine structure as observed in EDOT and ProDOT oligomers. Additionally, **AuNPs–DDA** absorbed up to 800 nm with a typical surface plasmon absorption (SPA) band around 530 nm. Since it is known that AuNPs with a diameter less than 2 nm lose the distinctive SPA band,[43] the synthesized **AuNPs–DDA** was confirmed to have a particle size of more than 2 nm. In contrast, for **2**, the vibrational fine structure of the maximum absorption band of the $E_2P_2$ moiety broadened with a 15 nm red-shift relative to that of **4c**. In addition, although no apparent SPA band was detected, the absorption edge reached 800 nm,

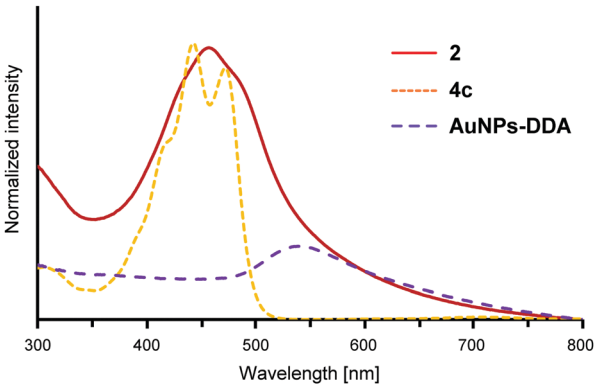


Fig. 2 Electronic absorption spectra of **2**, **4c**, and **AuNPs–DDA**.

similar to that of **AuNPs–DDA**. In the case of **1** (average particle size: 4.2 nm), a similar red-shift and absorption edge reaching the near-IR region was also observed, whereas SPA was identified as a shoulder band.[32] Collectively, the broad absorption maximum of **2** at 458 nm without shoulder peaks indicated that unreacted **4c** and uncoordinated species involving the neutral $E_2P_2$ moiety, such as the disulfide dimer, were sufficiently washed off. Furthermore, no apparent SPA band for **2** was observed, suggesting that the particle size of **2** decreased upon the ligand exchange reaction.

To characterize **2**, transmission electron microscopy (TEM) was conducted using a thin carbon film grid. As shown in Fig. 3a (for particle size and distribution, see Fig. S2, ESI†), the average particle size was observed to be 1.6 ± 0.5 nm. Thus, the decrease in particle size upon the ligand exchange reaction was confirmed. This is in sharp contrast to the result that the same ligand exchange of 2.5 nm **AuNPs–DDA** with 9-(4-mercaptophenylethynyl)anthracene appeared to retain the particle size.[42] The size decrease in **2** might be caused by the more bulky ProDOT unit with a diethyl side chain than the phenyl unit near the AuNP surface. The sterically demanding group near the AuNP surface, as utilized in the synthesis of gold nanoclusters,[44] could enlarge the curvature of the particles by steric repulsion. Furthermore, in our previous study, AuNPs covered with methylthio end-capped-terthiophene thiolate without substituents at the β-position showed a self-assembled structure probably owing to the interactions between the methythio group and neighboring AuNPs (Fig. 3b).[32] However, for AuNPs **1**, such an interaction was restricted due to the presence of the bulky bicyclo[2.2.2]octene unit at the β-position of thiophene rings[45] near the AuNP surface side. Similarly, no apparent self-assembled structure was observed in **2** as most particles were scattered. Thus, in the neutral state, the presence of the sterically demanding ProDOT units might also restrain the interparticle interaction between the outer methylthio group and Au atoms in the neighboring AuNPs.

Cyclic voltammetry (CV) of **2** (Fig. 4a) in $CH_2Cl_2$ containing 0.1 M tetrabutylammonium hexafluorophosphate ($TBAPF_6$) showed two couples of anodic and cathodic peaks. The averages of the first (−0.09 V (*vs.* $Fc/Fc^+$)) and second (+0.20 V (*vs.* $Fc/Fc^+$)) peaks ($E_{pa1}$ = −0.06 V, $E_{pc1}$ = −0.12 V; $E_{pa2}$ = +0.23 V, $E_{pc2}$ = +0.17 V) of **2** were slightly shifted to the positive potential side compared with those of **4a** ($E^{ox1}_{1/2}$ = −0.11 V, $E^{ox2}_{1/2}$ = +0.05 V

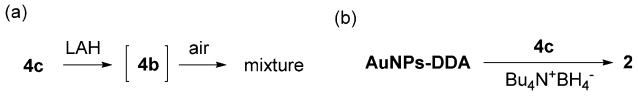


Scheme 2 Synthesis of AuNPs **2**.

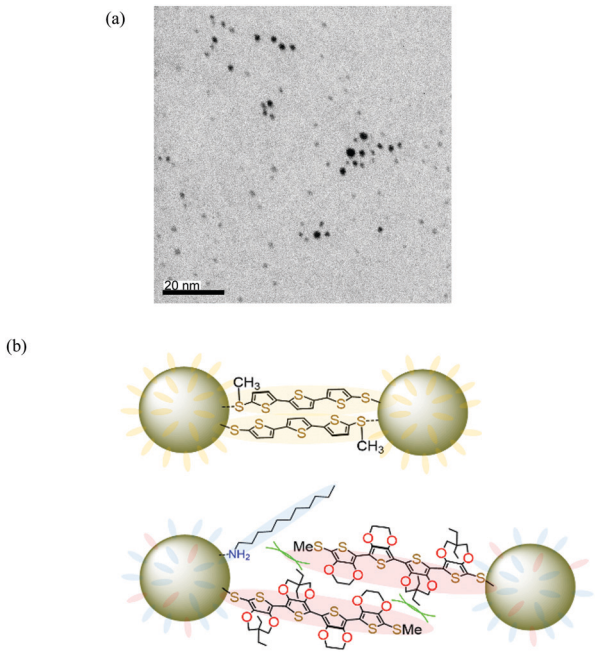


Fig. 3 (a) A TEM image of AuNPs **2**. (b) Schematic representations of the inter-particle interactions of AuNPs covered with methylthio end-capped terthiophene thiolate. In the case of **2**, such an interaction would be restricted.

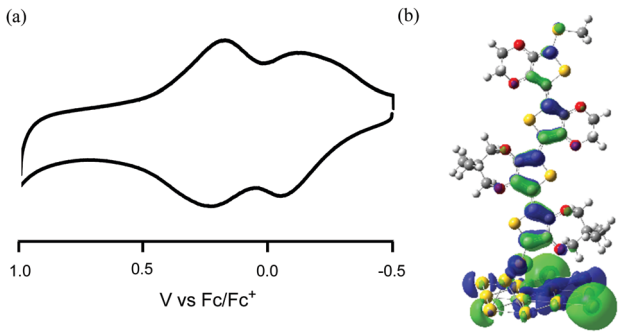


Fig. 4 (a) CV of **2** in $CH_2Cl_2$ with 0.1 M $TBAPF_6$. Scan rate: 0.1 V $s^{-1}$. (b) HOMO of $E_2P_2$ thiolate of the $Au_{13}$ cluster.

(*vs.* $Fc/Fc^+$)[28]), suggesting that the observed CV wave is due to the oxidation process of $E_2P_2$ moiety. To predict the HOMO level of **2**, DFT calculations of the single $E_2P_2$ thiolate on 12 (=3 × 4) Au atoms in a (111) arrangement and one Au adatom placed on a 2-fold hollow[46,47] were conducted using the M06 method (LanL2DZ for Au and 6-31G(d) for other elements). The calculated HOMO was spread on the $E_2P_2$ moiety (Fig. 4b) and the level (−4.72 eV) was almost identical to that of **4a** (−4.75 eV), supporting the interpretation of the results of CV. Furthermore, given the observation of anodic and cathodic couple at a low oxidation potential, the stable radical cation of the $E_2P_2$ moiety could be generated using a mild oxidizing agent.

The chemical one-electron oxidation of the $E_2P_2$ moiety on AuNPs **2** in $CH_2Cl_2$ was performed by adding a solution of $AgSbF_6$ until the absorption band due to the neutral $E_2P_2$ moiety disappeared. As shown in Fig. 5, two broad absorption bands appeared at 688 nm and ∼1140 nm owing to this oxidation reaction. These bands were similar to those of the radical cation **4a**$^{\bullet+}$ (717 nm, 1228 nm),[28] and therefore could be assigned to the SOMO–LUMO and HOMO–SOMO transitions of the radical cation of the $E_2P_2$ moiety on the AuNPs. No apparent diagnostic absorption bands for the π-dimer formation[28] between $E_2P_2$ moieties on the same AuNP surface was observed probably due to the repulsion between ProDOT units.

To confirm the presence of the radical cation moiety, an ESR spectrum was obtained. The oxidized **2** in $CH_2Cl_2$ exhibited a signal with a *g* value of 2.0028 at room temperature (Fig. S3, ESI†). The M06 calculations of the one-electron oxidized state of the single $E_2P_2$ thiolate of $Au_{13}$ (Fig. S4, ESI†) showed that the spin density is spread over the entire $E_2P_2$ and Au atoms, supporting the results of the UV-vis-NIR and ESR spectra.

A TEM image of the chemically oxidized **2** showed a self-assembled network structure over hundreds of nanometers (Fig. 6a) in contrast to the neutral **2** (Fig. 3a). The network seemed to be three-dimensionally linked; therefore, the average interparticle distance could not be determined. Nevertheless, in the enlarged image (Fig. 6b), some interparticle distances appeared to be ∼2 nm. The distances are comparable to that between the Au atom and the sulfur atom of the methylthio group in the calculated model as shown in Fig. S4 (ESI†). Collectively, these results suggest that the radical cation of the $E_2P_2$ moiety contributed to the enhancement of interparticle interactions, probably due to the radical cation π-dimer formation. However, the ratio of the π-dimerized $E_2P_2$ moiety compared to the free radical cation moiety on the AuNP surface was considered to be too small, leading to undetectable diagnostic absorption bands for the π-dimer formation.[28] However, based on the conductivity of the chemically oxidized **2** film, an interaction between the radical cation of the $E_2P_2$ moiety formed effective conduction paths.

## Conductivity of assembly of AuNPs 2 and their oxidized species

The conductivities of the drop-cast films of AuNPs **2** prepared from a dichloromethane solution were investigated. The IDA electrodes purchased were used for the measurements and, as reported previously,[32] the saturated values for the film dried after

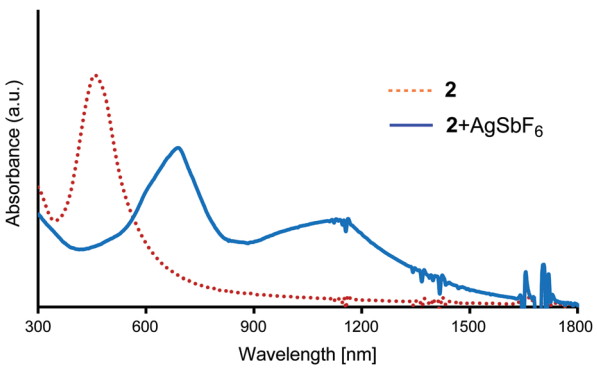


Fig. 5 Electronic absorption spectra of **2** oxidized with $AgSbF_6$.

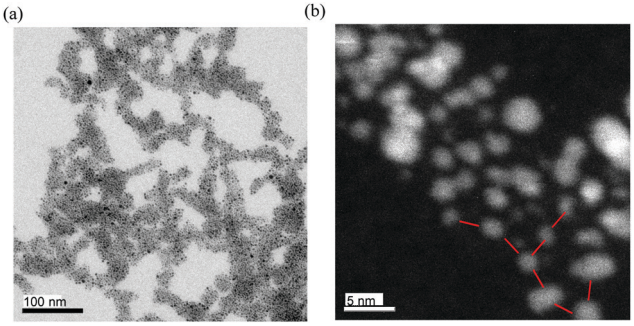


Fig. 6 (a) TEM image (500 × 500 nm) of chemically oxidized AuNPs **2** and (b) the enlarged image (black/white inverted for clarity). The red bars corresponding to the 2 nm scale are added to indicate interparticle distance.

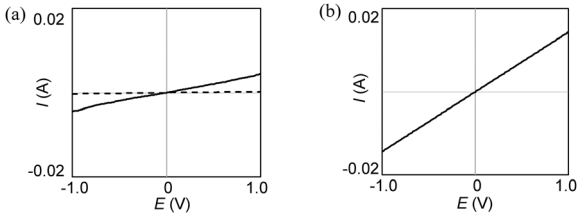


Fig. 7 A current–potential response of (a) the **2** film before (dashed line) and after $I_2$-doping (solid line) and (b) **2** + $AgSbF_6$ on an IDA electrode.

adding a few drops of solution[48] were considered. As described in the introduction, the conductivity of the drop-cast film of **1** was below the limit ($<10^{-6}$ S cm$^{-1}$) of the instrument used. Under the same measurement conditions, however, the conductivities of independently prepared two samples of neutral **2** with three repeated measurements ranged 1–2 × $10^{-4}$ S cm$^{-1}$ (Fig. 7a). Given that the length of the remaining DDA ligands (~1.5 nm) is shorter than that of $E_2P_2$ thiolate, **2** with a moderate molar fraction of DDA might allow closer proximity than **1**, which facilitates core-to-core tunneling conduction.[48]

The conductivities of the drop-cast films after doping using iodine vapor were enhanced, as observed in the case of AuNPs **1**. The $I_2$-doped films of **2** reached 5–9 × $10^{-3}$ S cm$^{-1}$, respectively. These values are comparable to those of the iodine-doped film of **1** (3.7 × $10^{-2}$ S cm$^{-1}$). Furthermore, the drop-cast films of **2** (independently prepared two samples) + $AgSbF_6$ had the same order of conductivity (1–3 × $10^{-2}$ S cm$^{-1}$) as shown in Fig. 7b. Comparing the iodine-doped and pre-oxidized films prepared from the same sample of **2**, the pre-oxidized film had better conductivity. Therefore, it can be concluded that the interparticle interaction between the $E_2P_2$ radical cation moieties on the neighboring AuNPs formed an effective conduction path. Judging from the inter-particle distance shown in Fig. 6b, the formation of a π-dimer between the radical cation moiety was most likely.

## Conclusions

In this study, we succeeded in the partial replacement of dodecylamine on AuNPs with methylthio end-capped EDOT and diethyl–ProDOT mixed tetramer $E_2P_2$ thiolate. The radical cation state of the $E_2P_2$ moiety on the AuNPs was stable in a dichloromethane solution at room temperature. The drop-cast film from this solution formed a self-assembled network structure over hundreds of nanometers. Based on the interparticle distance, a π-dimer between the radical cation moieties on the respective AuNPs were formed. To our knowledge, this is the first example of solution-processable AuNP assembly linked through the interaction between radical cations. The conductivity of the radical-cation-capped AuNP assembly was on the order of $10^{-2}$ S cm$^{-1}$, which was slightly better than that of the iodine-doped AuNP film. Although the conductivity was moderate possibly due to the limitation derived from the small particle size,[13] it can be concluded that the radical cation π-dimer was utilized to form effective conduction paths in the AuNP assembly.

## Conflicts of interest

There are no conflicts to declare.

## Acknowledgements

This work was supported by a Grant-in-Aid for Scientific Research (C) (No. 17K05977) from the Japan Society for the Promotion of Science (JSPS).

## References

1 M.-C. Daniel and D. Astruc, Gold nanoparticles: assembly, supramolecular chemistry, quantum-size-related properties, and applications toward biology, catalysis, and nanotechnology, *Chem. Rev.*, 2004, **104**, 293–346.
2 T. Ishida, T. Murayama, A. Taketoshi and M. Haruta, Importance of size and contact structure of gold nanoparticles for the genesis of unique catalytic processes, *Chem. Rev.*, 2020, **120**, 464–525.
3 Y. Ko, C. H. Kwon, S. W. Lee and J. Cho, Nanoparticle-based electrodes with high charge transfer efficiency through ligand exchange layer-by-layer assembly, *Adv. Mater.*, 2020, **32**, 1–26.
4 J. Olesiak-Banska, M. Waszkielewicz, P. Obstarczyk and M. Samoc, Two-photon absorption and photoluminescence of colloidal gold nanoparticles and nanoclusters, *Chem. Soc. Rev.*, 2019, **48**, 4087–4117.
5 K. Saha, S. S. Agasti, C. Kim, X. Li and V. M. Rotello, Gold nanoparticles in chemical and biological sensing, *Chem. Rev.*, 2012, **112**, 2739–2779.
6 D. A. Giljohann, D. S. Seferos, W. L. Daniel, M. D. Massich, P. C. Patel and C. A. Mirkin, Gold nanoparticles for biology and medicine, *Angew. Chem., Int. Ed.*, 2010, **49**, 3280–3294.
7 Y. Kim, J. Zhu, B. Yeom, M. Di Prima, X. Su, J.-G. Kim, S. J. Yoo, C. Uher and N. a. Kotov, Stretchable nanoparticle conductors with self-organized conductive pathways, *Nature*, 2013, **500**, 59–63.

8 T. Minari, Y. Kanehara, C. Liu, K. Sakamoto, T. Yasuda, A. Yaguchi, S. Tsukada, K. Kashizaki and M. Kanehara, Room-temperature printing of organic thin-film transistors with π-junction gold nanoparticles, *Adv. Funct. Mater.*, 2014, **24**, 4886–4892.
9 W. Huang, G. Masuda, S. Maeda, H. Tanaka and T. Ogawa, Molecular junctions composed of oligothiophene dithiol-bridged gold nanoparticles exhibiting photoresponsive properties, *Chem. – Eur. J.*, 2005, **12**, 607–619.
10 S. Taniguchi, M. Minamoto, M. M. Matsushita, T. Sugawara, Y. Kawada and D. Bethell, Electron transport in networks of gold nanoparticles connected by oligothiophene molecular wires, *J. Mater. Chem.*, 2006, **16**, 3459.
11 M. Ikeda, N. Tanifuji, H. Yamaguchi, M. Irie and K. Matsuda, Photoswitching of conductance of diarylethene-Au nanoparticle network, *Chem. Commun.*, 2007, 1355–1357.
12 K. Matsuda, H. Yamaguchi, T. Sakano, M. Ikeda, N. Tanifuji and M. Irie, Conductance photoswitching of diarylethene-gold nanoparticle network induced by photochromic reaction, *J. Phys. Chem. C*, 2008, **112**, 17005–17010.
13 G. Zotti, B. Vercelli and a. Berlin, Gold nanoparticles linked by pyrrole- and thiophene-based thiols. electrochemical, optical, and conductive properties, *Chem. Mater.*, 2008, **20**, 397–412.
14 M. Quintiliani, M. Bassetti, C. Pasquini, C. Battocchio, M. Rossi, F. Mura, R. Matassa, L. Fontana, M. V. Russo and I. Fratoddi, Network assembly of gold nanoparticles linked through fluorenyl dithiol bridges, *J. Mater. Chem. C*, 2014, **2**, 2517–2527.
15 T. Toyama, K. Higashiguchi, T. Nakamura, H. Yamaguchi, E. Kusaka and K. Matsuda, Photoswitching of conductance of diarylethene-gold nanoparticle network based on the alteration of π-conjugation, *J. Phys. Chem. Lett.*, 2016, **7**, 2113–2118.
16 B. C. Sih, A. Teichert and M. O. Wolf, Electrodeposition of oligothiophene-linked gold nanoparticle films, *Chem. Mater.*, 2004, **16**, 2712–2718.
17 N. Sun, S. Zhang, F. Simon, A. M. Steiner, J. Schubert, Y. Du, Z. Qiao, A. Fery and F. Lissel, Poly(3-hexylthiophene)s functionalized with *N*-heterocyclic carbenes as robust and conductive ligands for the stabilization of gold nanoparticles, *Angew. Chem., Int. Ed.*, 2021, **60**, 3912–3917.
18 M. Irie, T. Fukaminato, K. Matsuda and S. Kobatake, Photochromism of diarylethene molecules and crystals: memories, switches, and actuators, *Chem. Rev.*, 2014, **114**, 12174–12277.
19 T. Nishinaga and K. Komatsu, Persistent π radical cations: self-association and its steric control in the condensed phase, *Org. Biomol. Chem.*, 2005, **3**, 561–569.
20 D.-W. Zhang, J. Tian, L. Chen, L. Zhang and Z.-T. Li, Dimerization of conjugated radical cations: an emerging non-covalent interaction for self-assembly, *Chem. – Asian J.*, 2015, **10**, 56–68.
21 L. L. Miller and K. R. Mann, π-Dimers and π-stacks in solution and in conducting polymers, *Acc. Chem. Res.*, 1996, **29**, 417–423.
22 D. D. Graf, R. G. Duan, J. P. Campbell, L. L. Miller and K. R. Mann, From monomers to π-stacks. a comprehensive study of the structure and properties of monomeric, π-dimerized, and π-stacked forms of the cation radical of 3′,4′-dibutyl-2,5″-diphenyl-2,2′:5′,2″-terthiophene, *J. Am. Chem. Soc.*, 1997, **119**, 5888–5899.
23 T. Nishinaga, in *Organic Redox Systems*, ed. T. Nishinaga, Wiley, 2016, pp. 383–410.
24 D. Yamazaki, T. Nishinaga, N. Tanino and K. Komatsu, Terthiophene radical cations end-capped by bicyclo[2.2.2]-octene units: formation of bent π-dimers mutually attracted at the central position, *J. Am. Chem. Soc.*, 2006, **128**, 14470–14471.
25 M. Tateno, M. Takase, M. Iyoda, K. Komatsu and T. Nishinaga, Steric control in the π-dimerization of oligothiophene radical cations annelated with bicyclo[2.2.2]octene units, *Chem. – Eur. J.*, 2013, **19**, 5457–5467.
26 T. Nishinaga, T. Kageyama, M. Koizumi, K. Ando, M. Takase and M. Iyoda, Effect of substituents on the structure, stability, and π-dimerization of dithienylpyrrole radical cations, *J. Org. Chem.*, 2013, **78**, 9205–9213.
27 M. Hasegawa, K. Kobayakawa, H. Matsuzawa, T. Nishinaga, T. Hirose, K. Sako and Y. Mazaki, Macrocyclic oligothiophene with stereogenic [2.2]paracyclophane scaffolds: chiroptical properties from π-transannular interactions, *Chem. – Eur. J.*, 2017, **23**, 3267–3271.
28 T. Nishinaga and Y. Sotome, Stable radical cations and their π-dimers prepared from ethylene- and propylene-3,4-dioxythiophene co-oligomers: combined experimental and theoretical investigations, *J. Org. Chem.*, 2017, **82**, 7245–7253.
29 T. Akahane, M. Takase, Y. Mazaki and T. Nishinaga, π-Dimerization ability of conjugated oligomer dication diradicaloids composed of dithienylpyrrole and benzodithiophene units, *Heteroat. Chem.*, 2018, **29**, 1–8.
30 T. Nishinaga, Y. Kanzaki, D. Shiomi, K. Matsuda, S. Suzuki and K. Okada, Radical cation π-dimers of conjugated oligomers as molecular wires: an analysis based on nitronyl nitroxide spin labels, *Chem. – Eur. J.*, 2018, **24**, 11717–11728.
31 T. Fujiwara, A. Muranaka, T. Nishinaga, S. Aoyagi, N. Kobayashi, M. Uchiyama, H. Otani and M. Iyoda, Preparation, spectroscopic characterization and theoretical study of a three-dimensional conjugated 70 π-electron thiophene 6-mer radical cation π-dimer, *J. Am. Chem. Soc.*, 2020, **142**, 5933–5937.
32 M. Tateno, M. Takase and T. Nishinaga, Synthesis and conductive properties of gold nanoparticles protected by partially bicyclo[2.2.2]octene-annelated and methylthio end-capped oligothiophene thiolates, *Chem. Mater.*, 2014, **26**, 3804–3810.
33 J. J. Apperloo, L. B. Groenendaal, H. Verheyen, M. Jayakannan, R. a J. Janssen, A. Dkhissi, D. Beljonne, R. Lazzaroni and J.-L. Brédas, Optical and redox properties of a series of 3,4-ethylenedioxythiophene oligomers, *Chem. – Eur. J.*, 2002, **8**, 2384–2396.
34 P. M. Burrezo, B. Pelado, R. P. Ortiz, P. De La Cruz, J. T. L. Navarrete, F. Langa and J. Casado, Robust

ethylenedioxythiophene-vinylene oligomers from fragile thiophene-vinylene cores: Synthesis and optical, chemical and electrochemical properties of multicharged shapes, *Chem. – Eur. J.*, 2015, **21**, 1713–1725.

35 C. Lin, T. Endo, M. Takase, M. Iyoda and T. Nishinaga, Structural, optical, and electronic properties of a series of 3,4-propylenedioxythiophene oligomers in neutral and various oxidation states, *J. Am. Chem. Soc.*, 2011, **133**, 11339–11350.

36 N. B. Teran and J. R. Reynolds, Discrete donor-acceptor conjugated systems in neutral and oxidized states: implications toward molecular design for high contrast electrochromics, *Chem. Mater.*, 2017, **29**, 1290–1301.

37 A. Zabet-Khosousi and A.-A. Dhirani, Charge transport in nanoparticle assemblies, *Chem. Rev.*, 2008, **108**, 4072–4124.

38 P. M. Beaujuge and J. R. Reynolds, Color control in π-conjugated organic polymers for use in electrochromic devices, *Chem. Rev.*, 2010, **110**, 268–320.

39 N. G. Connelly and W. E. Geiger, Chemical redox agents for organometallic chemistry, *Chem. Rev.*, 1996, **96**, 877–910.

40 K. Takagi, H. Takachi and K. Sasaki, Syntheses of organic n,n-dialkyldithiocarbamates or organic thiocyanates from organozincs and corresponding thio-anions via the inversion of electronic reactivity of the anions with NCS-oxidation, *J. Org. Chem.*, 1995, **60**, 6552–6556.

41 M. Brust, M. Walker, D. Bethell, D. J. Schiffrin and R. Whyman, Synthesis of thiol-derivatised gold nanoparticles in a two-phase liquid-liquid system, *J. Chem. Soc., Chem. Commun.*, 1994, 801–802.

42 T. Zdobinsky, P. Sankar Maiti and R. Klajn, Support curvature and conformational freedom control chemical reactivity of immobilized species, *J. Am. Chem. Soc.*, 2014, **136**, 2711–2714.

43 Y. G. Kim, S. K. Oh and R. M. Crooks, Preparation and characterization of 1-2 nm dendrimer-encapsulated gold nanoparticles having very narrow size distributions, *Chem. Mater.*, 2004, **16**, 167–172.

44 R. Jin, Quantum sized, thiolate-protected gold nanoclusters, *Nanoscale*, 2010, **2**, 343–362.

45 T. Nishinaga, A. Wakamiya, D. Yamazaki and K. Komatsu, Crystal structures and spectroscopic characterization of radical cations and dications of oligothiophenes stabilized by annelation with bicyclo[2.2.2]octene units: sterically segregated cationic oligothiophenes, *J. Am. Chem. Soc.*, 2004, **126**, 3163–3174.

46 E. Pensa, E. Cortés, G. Corthey, P. Carro, C. Vericat, M. H. Fonticelli, G. Benítez, A. a. Rubert and R. C. Salvarezza, The chemistry of the sulfur-gold interface: in search of a unified model, *Acc. Chem. Res.*, 2012, **45**, 1183–1192.

47 P. D. Jadzinsky, G. Calero, C. J. Ackerson, D. a. Bushnell and R. D. Kornberg, Structure of a thiol monolayer-protected gold nanoparticle at 1.1 A resolution, *Science*, 2007, **318**, 430–433.

48 W. P. Wuelfing, S. J. Green, J. J. Pietron, D. E. Cliffel and R. W. Murray, Electronic conductivity of solid-state, mixed-valent, monolayer-protected au clusters, *J. Am. Chem. Soc.*, 2000, **122**, 11465–11472.